Buckybowls

DOI: 10.1002/anie.201002515

The Bicorannulenyl Dianion: A Charged Overcrowded Ethylene**

*David Eisenberg, Edward A. Jackson, Jennifer M. Quimby, Lawrence T. Scott, and Roy Shenhar**

The interplay between structural strain and conjugation makes two families of polycyclic hydrocarbons—buckybowls[1] and overcrowded ethylenes (OEs)[2]—particularly appealing. This interplay gives rise to a rich stereochemistry in OEs, and allows buckybowls, which are polycyclic hydrocarbons that can be mapped onto fullerene surfaces, to be used as model compounds[1,3] and possible precursors[4] for curved carbon-rich structures such as fullerenes and carbon nanotubes.[2] Buckybowls are also interesting because of their organometallic[5] and supramolecular[6] chemistry, photophysical properties,[7] and reduction capacity.[8,9] Corannulene ($C_{20}H_{10}$), the archetypal buckybowl, is the smallest curved subunit of C_{60}.[1] Corannulene can accept several negative charges because of the double degeneracy of its lowest unoccupied molecular orbital (LUMO), which arises from its high symmetry. Reduction of corannulene and other buckybowls often leads to unusual structural and electronic phenomena,[8] such as anisotropic charge redistribution[10] and self-assembly through different binding modes.[11]

The stereochemistry of OEs has fascinated chemists for over a century[12] and has promoted the return of OEs to the spotlight of material science as structural elements in molecular machines and switches.[2,13] OEs can be interconverted between the principal conformations, that is, folded and twisted, by applying external stimuli, such as heat,[12,14] pressure,[12,15] photoexcitation,[14] and redox chemistry.[16] To the best of our knowledge, in every OE studied so far, reduction or oxidation relieves the steric hindrance present in the neutral molecule by decreasing the conjugation between the two units, thus effectively converting the OE into a twisted biaryl unit.[16,17] An elegant exploitation of this property for switching was demonstrated by Feringa and coworkers, where a redox reaction of a bithiaxanthylidene derivative served as input in a three-state luminescent switch.[18] The opposite phenomenon, where reduction of a biaryl unit increases the double-bond character of the tether connecting the two subunits is extremely rare and has only been demonstrated so far in small molecules, such as biphenyl and 1,1′-binaphthyl.[19]

Herein we describe the alkali-metal reduction of bicorannulenyl (**1**), a large biaryl composed of two corannulene units, and demonstrate that the single bond tethering the two corannulene units acquires a substantial double-bond character upon charging to a dianion, thus effectively transforming **1** into a charged OE (Scheme 1).

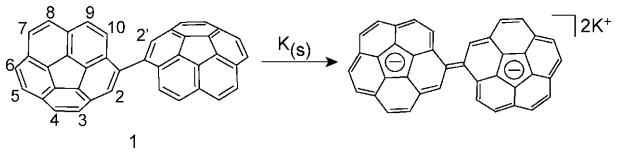

Scheme 1. Reduction of bicorannulenyl (**1**) with elemental potassium.

The dynamic stereochemistry of neutral **1** has been recently elucidated by our research group.[20] Compound **1** contains two chiral elements: the asymmetry of a monosubstituted corannulenyl bowl, and the helical chirality around the central bond. Together, these elements give rise to rich stereodynamics. The neutral molecule displays twelve stable conformations, but because of the low energy barrier for breaking the π conjugation between the units (1–2 kcal mol^{-1}, similar to biphenyl),[21] only three chiral diastereomers (three pairs of enantiomers) are observed in the ^{1}H NMR spectrum. The diastereomers interconvert through bowl-to-bowl inversions and rotations about the central bond. To facilitate the discussion, each conformation is annotated according to the following conventions: R/S for right or left twist of the tether; P/M for the handedness of the bowls; and a subscript number denoting the twist angle. Thus, enantiomers would have inverse annotations, for example, S.PP$_{139}$ and R.MM$_{-139}$.

When bicorannulenyl is reduced by using potassium metal in [D$_8$]THF,[22] a diamagnetic species is observed in the ^{1}H NMR spectrum at low temperatures (Figure 1). The spectrum at 190 K consists of two sets of absorptions spread over a range of $\Delta = 6$ ppm, each with one singlet and eight doublet signals, with a relative integration ratio of 3.8:1. As the temperature is increased, the spectrum disappears reversibly without change in chemical shifts, thus indicating rapid equilibrium with a thermally accessible triplet spin state.[23] 2D NMR experiments (COSY and NOESY) indicate that the two sets of signals represent two separate diastereomers that interconvert on the NMR timescale. All ^{1}H and ^{13}C NMR

[*] D. Eisenberg, Dr. R. Shenhar
Institute of Chemistry and the Lise Meitner-Minerva Center for Computational Quantum Chemistry, The Hebrew University Jerusalem, 91904 (Israel)
Fax: (+972) 2-658-5345
E-mail: roys@chem.ch.huji.ac.il
Homepage: http://chem.ch.huji.ac.il/shenhar-group
Dr. E. A. Jackson, J. M. Quimby, Prof. Dr. L. T. Scott
Department of Chemistry, Merkert Chemistry Center
Boston College
Chestnut Hill, MA 02467 (USA)

[**] Financial support from the National Science Foundation (NSF) and from The Lise Meitner-Minerva Center for Computational Quantum Chemistry is gratefully acknowledged.

Supporting information for this article is available on the WWW under http://dx.doi.org/10.1002/anie.201002515.

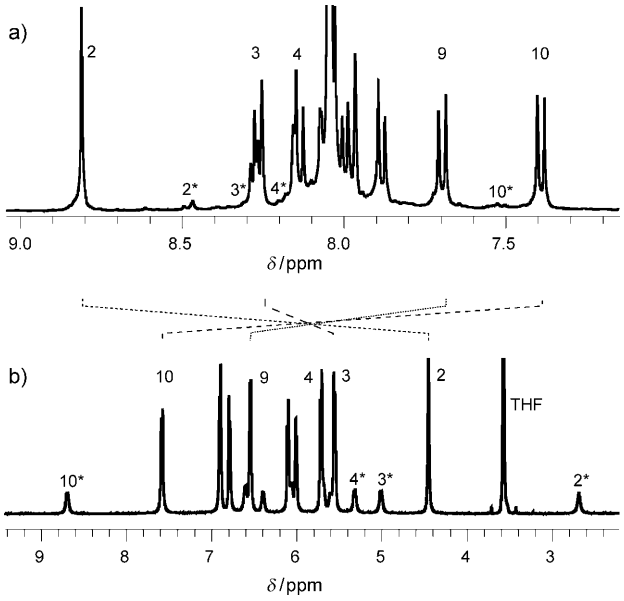

Figure 1. ^{1}H NMR spectra of a) **1** and b) $\mathbf{1}^{2-}$ at 190 K. Representative signals are annotated (see Scheme 1 for numbers, minor isomer signals are marked with *). Note the change in the spectral range.

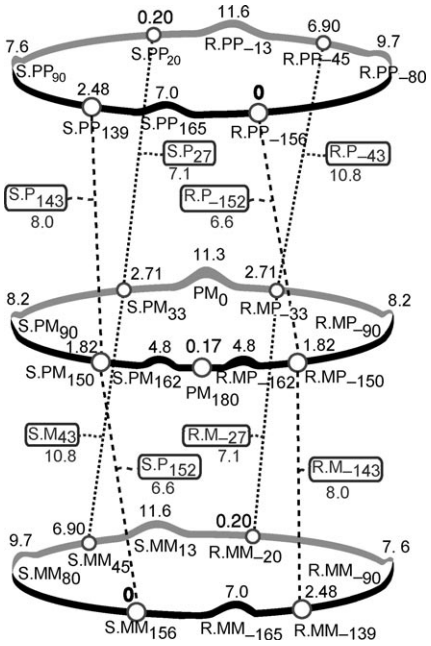

Figure 2. Stereodynamics map for $\mathbf{1}^{2-}$. Stable conformations are represented by circles. Dotted lines represent bowl-inversion pathways, and the labels on these lines represent the transition states and their energies. The numbers represent calculated Gibbs free energies in kcal mol^{-1} relative to the lowest energy conformation $S.MM_{156}/R.PP_{-156}$ at 190 K.

signals were assigned for the major isomer (assisted by theoretical calculations; see below). The full assignment reveals a complete reversal of signal ordering relative to the ^{1}H NMR of diatropic neutral **1**, hence demonstrating a strong paratropic ring current in the anion (Figure 1).

When this anion is reduced further, the well-defined ^{1}H NMR spectrum disappears and a weak broad signal appears at around $\delta = -3.7$ ppm (200 K).[24] This high-field signal is typical for the antiaromatic corannulene dianion,[8b] and identifies the second reduction state of bicorannulenyl as a tetraanion with two additional electrons in each corannulenyl bowl. This result allows us to conclude that the first reduction state, which is in the focus of the work presented herein, is a dianion. To verify this hypothesis, we calculated the ^{13}C NMR chemical shifts of all possible minimum energy conformations of the dianion and tetraanion at the DFT level and compared them to the experimental assignment.[24] The calculated chemical shifts are consistent with the charge assignment of a dianion. The calculations show an average chemical shift difference between calculated and observed values of less than 12 ppm for all computed conformations of the dianion, compared to a difference greater than 25 ppm for the most stable conformation of the tetraanion.[24]

Having identified the reduction state of the observed species, the two sets of signals were assigned to the appropriate conformations of the bicorannulenyl dianion. Based on the chiral elements of bicorannulenyl mentioned above, its stereochemistry can be represented on the face of a cylinder (Figure 2).[20] On this stereodynamics map, the vertical axis denotes bowl-to-bowl inversion, and the circular axis denotes a 360° rotation around the central bond. *E* isomers appear on the front face of the cylindrical map, and *Z* isomers appear in the back.

The geometries were optimized, and their energies and vibration frequencies were computed for all thirteen minimum-energy conformations found, as well as for the transition states that arise from the bowl-to-bowl inversions (e.g., $S.P_{143}$), sterically hindered rotations around the central bond (e.g., $S.PP_{165}$), and *E*/*Z* isomerizations (e.g., $S.PP_{90}$). The thirteen stable conformations are divided into six pairs of enantiomers, and a single achiral isomer (PM_{180}).

Gas-phase calculations predict three stable diastereomers (PM_{180}, $S.MM_{156}/R.PP_{-156}$, and $S.PP_{20}/R.MM_{-20}$), out of the seven possible stereoisomeric conformations. However, the ^{1}H NMR spectrum shows only two sets of signals. This discrepancy can be explained by a fast exchange between two of the most stable diastereomeric conformations, thus producing a single set of absorptions that represents an average conformation. Because all gas-phase-calculated energy barriers are of similar magnitude (5–10 kcal mol^{-1}), and since the neglected ion pairing and the solvation further modify the potential energy surface of the conformational dynamics, it is impossible to decide which exchange pathway is faster, and thus to assign NMR absorptions unequivocally. However, the calculated spectrum of the PM_{180} isomer fits best to the experimental ^{13}C NMR chemical shifts of the major isomer,[24] thus suggesting that PM_{180} might be the major isomer in solution.

By using exchange NMR spectroscopy (EXSY),[24,25] we have measured the rates of the chemical exchange between the two observed isomers at 190 K. Based on these rates, the energy barrier for conversion of the major isomer into the minor isomer was calculated to be $\Delta G^{\ddagger}_{190K} = (11.1 \pm 0.1)$ kcal mol^{-1} by using the Eyring equation[26]. According to the stereochemical analysis (Figure 2), this barrier must arise

from two consecutive conformational changes, that is, either a combination of bowl inversion and bond rotation, or two consecutive bond rotations.

The most important observation from the computational results is that in the calculated geometries of the $\mathbf{1}^{2-}$ isomers, the central bond becomes shorter and the central twist angle is flattened compared to both neutral **1** and $\mathbf{1}^{4-}$ (Table 1).

Table 1: Calculated lengths and twist angles of the central bond.[a]

Central bond	$\mathbf{1}^{[20]}$ S.PP$_{44}$	S.PM$_{58}$	S.MM$_{137}$	$\mathbf{1}^{2-}$ S.PP$_{20}$	PM$_{180}$	S.MM$_{156}$	$\mathbf{1}^{4-}$ S.MM$_{147}$
length [Å]	1.482	1.484	1.480	1.431	1.410	1.432	1.494
twist angle [°]	44.4	57.5	137.0	19.7	180.0	155.7	147.0

[a] Calculations performed at the PBE0/6-31G* level. Only stable isomers ($\Delta G < 2$ kcal mol^{-1} relative to others) are considered.

Table 2: Bond order alternation in neutral **1** and its anionic species.[a]

Bond	$\mathbf{1}^{[20]}$ Bond lengths S.PP$_{44}$	S.PM$_{58}$	S.MM$_{137}$	$^1J_{HH}$	$\mathbf{1}^{2-}$ Bond lengths S.PP$_{20}$	PM$_{180}$	S.MM$_{156}$	$^1J_{HH}$	$\mathbf{1}^{4-}$ Bond lengths S.MM$_{147}$
a	1.394	1.395	1.395		1.459	1.463	1.453		1.398
b	1.384	1.385	1.385	8.7	1.382	1.378	1.382	9.0	1.451
c	1.385	1.386	1.385	8.8	1.412	1.410	1.416	7.5	1.414
d	1.385	1.386	1.384	8.7	1.392	1.385	1.388	8.6	1.405
e	1.385	1.386	1.386	8.9	1.397	1.405	1.403	7.7	1.450

[a] Calculated bond lengths ([Å]; PBE0/6-31G*) and experimental $^1J_{HH}$ coupling constants (Hz, major isomer) along the periphery of the bowls in neutral, di-, and tetraanionic bicorannulenyl.

Additionally, the energy barriers for the *E*/*Z* isomerization are significantly higher in the dianion (8–10 kcal mol^{-1}) than in the neutral compound (1–2 kcal mol^{-1}, similar to that of biphenyl).[20,21] These results suggest an increase in bond order for the tether in $\mathbf{1}^{2-}$. Each bowl bears an additional electron, thus rendering the bowls equivalent in the NMR spectra and reversing the ring current to paratropic. This species is a closed-shell singlet system at low temperatures; an increase in temperature populates the close-lying triplet state.[23]

Further support for the dianionic structure shown in Scheme 1 is obtained from bond-order considerations. Interestingly, in all Lewis resonance structures of a dianion with a central double bond, the bond orders on the rim (a–e, Scheme 2) are fixed at their positions, and alternate from single to double along the rim of each bowl. Bond length alternation was indeed observed in the DFT-level calculated isomers of $\mathbf{1}^{2-}$ but not in **1** or $\mathbf{1}^{4-}$ (Table 2). Compelling experimental evidence for this model comes from the strong alternation of the $^1J_{HH}$ coupling constants along the periphery of the bowl (Table 2), thus supporting the theoretically predicted trend. This alternation upholds the hypothesis that the central bond has significant double-bond character, because only a double bond between the bowls would fix the bond orders on the rim in the observed manner.

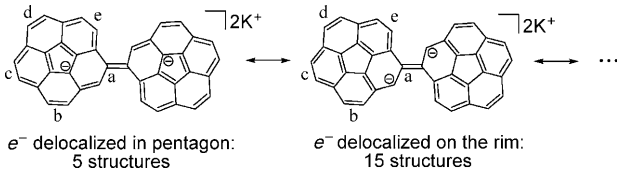

Scheme 2. Possible resonance Lewis structures of $\mathbf{1}^{2-}$. The number of structures is calculated for one additional electron in each bowl.

A simplistic "annulene-within-an-annulene" model predicts that the added electron resides on the pentagon of each bowl and renders it aromatic with six π electrons (a Hückel number). However, according to a higher-level charge distribution analysis obtained with natural population analysis (PBE0/6-311G**),[24,27] most of the charge is located on the periphery of the bowl. The strong anisotropy of the system, which is evident from the strong paratropic ring current, prevented us from obtaining a reliable experimental charge distribution from the differences in the ^{13}C NMR signals. The calculated charge distribution in $\mathbf{1}^{2-}$ is similar to that of other corannulene anions, in which excess charge is usually distributed on the rim,[10c,d,28] probably to minimize Coulombic repulsion within each bowl.

The change in bond order observed in $\mathbf{1}^{2-}$ can be rationalized with a frontier molecular orbital analysis. While the highest occupied molecular orbital (HOMO) of the neutral molecule features an antibonding π overlap along the tether (Figure 3a), the HOMO of the dianion features a clear bonding interaction (Figure 3b), which contributes to the double-bond character.

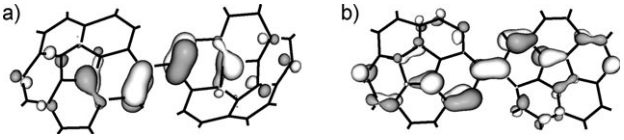

Figure 3. HOMOs of a) **1** (S.MM$_{137}$) and b) $\mathbf{1}^{2-}$ (PM$_{180}$; PBE0/6-311G**).

In several small biaryl molecules that exhibit an increase in bond order of the tether upon reduction, the LUMO also features a localized double-bond character on the central bond.[19] The transformation occurs in $\mathbf{1}^{2-}$, despite the overcrowded 1,1′-binaphthyl moiety that can be traced on its skeleton, and probably occurs with greater ease than in 1,1′-binaphthyl itself[19b] because of the curvature introduced by the corannulene bowls. The curvature minimizes the mutual steric repulsion by removing the protons situated on both sides of the tether from its plane in opposite directions. When the molecule adopts the PM$_{180}$ conformation in which the bowls face opposite directions (C_i symmetry; Figure 4) the steric crowding is minimized while the double-bond character of the central bond can retain its planarity in this conformation (Table 1).

Figure 4. The PM_{180} conformation of $\mathbf{1}^{2-}$ (PBE0/6-31G*).

In addition to the molecular orbital rationalization, other driving forces for the enhanced double-bond character of the tether might be involved. One is the increased resonance energy, gained from improved conjugation between the bowls and resulting in electron delocalization over a particularly large system. The other driving force is the avoidance of antiaromaticity—in the alternative charge distribution model for $\mathbf{1}^{2-}$, two electrons are delocalized on one bowl (undergoing charge hopping[29] to the other, neutral bowl), thus rendering it unfavorably antiaromatic.[8b] Overall, the dianion avoids this situation by becoming a conjugated, closed-shell system with a localized double-bond tether.

To summarize, it was found that upon converting neutral bicorannulenyl to a dianion, the central bond assumes double-bond character. This transformation of a large biaryl system to an overcrowded ethylene is especially impressive because of the anticipated steric crowding of the central bond, around which there is a 1,1′-binaphthyl substructure. The crowding is effectively avoided by the introduction of a curved element, the corannulene bowl. Evidence for this transformation was provided by theoretical calculations and corroborated experimentally by NMR spectroscopy, which shows a clear bond alternation pattern at the rim of the bicorannulenyl dianion. The stereochemistry of this special charged overcrowded ethylene was also described with the help of a combined theoretical and experimental approach. We anticipate that the introduction of the corannulene functionality into the area of overcrowded ethylenes and molecular machinery will serve to advance new functionality in the field.

Received: April 27, 2010
Published online: September 2, 2010

Keywords: annulenes · carbanions · conformation analysis · conjugation · overcrowded ethylenes

[1] a) L. T. Scott, *Pure Appl. Chem.* **1996**, *68*, 291 – 300; b) P. W. Rabideau, A. Sygula, *Acc. Chem. Res.* **1996**, *29*, 235 – 242; c) Y.-T. Wu, J. S. Siegel, *Chem. Rev.* **2006**, *106*, 4843 – 4867; d) A. Sygula, P. W. Rabideau in *Carbon-Rich Compounds: From Molecules to Materials* (Eds.: M. M. Haley, R. R. Tykwinski), Wiley-VCH, Weinheim, **2006**, pp. 529 – 565; e) V. M. Tsefrikas, L. T. Scott, *Chem. Rev.* **2006**, *106*, 4868 – 4884.

[2] a) P. U. Biedermann, J. J. Stezowski, I. Agranat in *Advances in Theoretically Interesting Molecules*, *Vol. 4* (Ed.: R. P. Thummel), JAI, Stamford, Connecticut, **1998**, pp. 245 – 322; b) B. L. Feringa, *Acc. Chem. Res.* **2001**, *34*, 504 – 513; c) B. L. Feringa, *J. Org. Chem.* **2007**, *72*, 6635 – 6652.

[3] a) K. K. Baldridge, J. S. Siegel, *Theor. Chem. Acc.* **1997**, *97*, 67 – 71; b) G. N. Sastry, *J. Mol. Struct.* **2006**, *771*, 141 – 147, and references therein.

[4] a) L. T. Scott, M. M. Boorum, B. J. McMahon, S. Hagen, J. Mack, J. Blank, H. Wegner, A. de Meijere, *Science* **2002**, *295*, 1500 – 1503; b) B. D. Steinberg, E. A. Jackson, A. S. Filatov, A. Wakamiya, M. A. Petrukhina, L. T. Scott, *J. Am. Chem. Soc.* **2009**, *131*, 10537 – 10545; c) Y. Ohta, Y. Okamoto, S. Irle, K. Morokuma, *Phys. Rev. B* **2009**, *79*, 195415.

[5] a) M. A. Petrukhina, L. T. Scott, *Dalton Trans.* **2005**, 2969 – 2975; b) M. A. Petrukhina, *Coord. Chem. Rev.* **2007**, *251*, 1690 – 1698; c) R. Maag, B. H. Northrop, A. Butterfield, A. Linden, O. Zerbe, Y. M. Lee, K. W. Chi, P. J. Stang, J. S. Siegel, *Org. Biomol. Chem.* **2009**, *7*, 4881 – 4885; d) A. S. Filatov, A. Y. Rogachev, E. A. Jackson, L. T. Scott, M. A. Petrukhina, *Organometallics* **2010**, *29*, 1231 – 1237.

[6] a) A. Sygula, F. R. Fronczek, R. Sygula, P. W. Rabideau, M. M. Olmstead, *J. Am. Chem. Soc.* **2007**, *129*, 3842 – 3843; b) A. J. Olson, Y. H. E. Hu, E. Keinan, *Proc. Natl. Acad. Sci. USA* **2007**, *104*, 20731 – 20736; c) W. Xiao, D. Passerone, P. Ruffieux, K. Ait-Mansour, O. Groning, E. Tosatti, J. S. Siegel, R. Fasel, *J. Am. Chem. Soc.* **2008**, *130*, 4767 – 4771; d) A. Sygula, S. Saebo, *Int. J. Quantum Chem.* **2009**, *109*, 65 – 72.

[7] a) R. Shenhar, I. Willner, D. V. Preda, L. T. Scott, M. Rabinovitz, *J. Phys. Chem. A* **2000**, *104*, 10631 – 10636; b) M. Yamaji, K. Takehira, T. Mikoshiba, S. Tojo, Y. Okada, M. Fujitsuka, T. Majima, S. Tobita, J. Nishimura, *Chem. Phys. Lett.* **2006**, *425*, 53 – 57; c) J. Mack, P. Vogel, D. Jones, N. Kaval, A. Sutton, *Org. Biomol. Chem.* **2007**, *5*, 2448 – 2452; d) Y. Matsuo, Y. Sato, M. Hashiguchi, K. Matsuo, E. Nakamura, *Adv. Funct. Mater.* **2009**, *19*, 2224 – 2229.

[8] a) A. Ayalon, M. Rabinovitz, P. C. Cheng, L. T. Scott, *Angew. Chem.* **1992**, *104*, 1691 – 1692; *Angew. Chem. Int. Ed. Engl.* **1992**, *31*, 1636 – 1637; b) M. Baumgarten, L. Gherghel, M. Wagner, A. Weitz, M. Rabinovitz, P. C. Cheng, L. T. Scott, *J. Am. Chem. Soc.* **1995**, *117*, 6254 – 6257.

[9] a) I. Aprahamian, M. Rabinovitz in *The Chemistry of Organolithium Compounds*, *Vol. 2* (Eds.: Z. Rappoport, I. Marek), Wiley, Chichester, **2006**, pp. 477 – 524; b) T. Sternfeld, M. Rabinovitz in *Carbon Rich Compounds: from Molecules to Materials* (Eds.: M. M. Haley, R. R. Tykwinski), Wiley-VCH, Weinheim, **2006**, pp. 566 – 623.

[10] a) A. Weitz, E. Shabtai, M. Rabinovitz, M. S. Bratcher, C. C. McComas, M. D. Best, L. T. Scott, *Chem. Eur. J.* **1998**, *4*, 234 – 239; b) H. Sakurai, T. Daiko, H. Sakane, T. Amaya, T. Hirao, *J. Am. Chem. Soc.* **2005**, *127*, 11580 – 11581; c) I. Aprahamian, D. V. Preda, M. Bancu, A. P. Belanger, T. Sheradsky, L. T. Scott, M. Rabinovitz, *J. Org. Chem.* **2006**, *71*, 290 – 298; d) S. Nishida, Y. Morita, A. Ueda, T. Kobayashi, K. Fukui, K. Ogasawara, K. Sato, T. Takui, K. Nakasuji, *J. Am. Chem. Soc.* **2008**, *130*, 14954 – 14955.

[11] a) A. Ayalon, A. Sygula, P.-C. Cheng, M. Rabinovitz, P. W. Rabideau, L. T. Scott, *Science* **1994**, *265*, 1065 – 1067; b) R. Shenhar, H. Wang, R. E. Hoffman, L. Frish, L. Avram, I. Willner, A. Rajca, M. Rabinovitz, *J. Am. Chem. Soc.* **2002**, *124*, 4685 – 4692; c) I. Aprahamian, R. E. Hoffman, T. Sheradsky, D. V. Preda, M. Bancu, L. T. Scott, M. Rabinovitz, *Angew. Chem.* **2002**, *114*, 1788 – 1791; *Angew. Chem. Int. Ed.* **2002**, *41*, 1712 – 1715; d) I. Aprahamian, D. Eisenberg, R. E. Hoffman, T. Sternfeld, Y. Matsuo, E. A. Jackson, E. Nakamura, L. T. Scott, T. Sheradsky, M. Rabinovitz, *J. Am. Chem. Soc.* **2005**, *127*, 9581 – 9587; e) N. Treitel, T. Sheradsky, L. Peng, L. T. Scott, M. Rabinovitz, *Angew. Chem.* **2006**, *118*, 3351 – 3355; *Angew. Chem. Int. Ed.* **2006**, *45*, 3273 – 3277.

[12] a) H. Meyer, *Monatsh. Chem.* **1909**, *30*, 165 – 177; b) H. Meyer, *Ber. Dtsch. Chem. Ges. B* **1909**, *42*, 143 – 145.

[13] a) G. S. Kottas, L. I. Clarke, D. Horinek, J. Michl, *Chem. Rev.* **2005**, *105*, 1281 – 1376; b) W. R. Browne, B. L. Feringa, *Nat. Nanotechnol.* **2006**, *1*, 25 – 35; c) E. R. Kay, D. A. Leigh, F. Zerbetto, *Angew. Chem.* **2007**, *119*, 72 – 196; *Angew. Chem. Int. Ed.* **2007**, *46*, 72 – 191.

[14] a) E. D. Bergmann, *Prog. Org. Chem.* **1955**, *3*, 81 – 171; b) M. K. J. ter Wiel, M. G. Kwit, A. Meetsma, B. L. Feringa, *Org. Biomol. Chem.* **2007**, *5*, 87 – 96; c) E. Fischer, *Rev. Chem.*

Intermed. **1984**, *5*, 393 – 422; d) J. Wang, A. Kulago, W. Browne, B. L. Feringa, *J. Am. Chem. Soc.* **2010**, *132*, 4191 – 4196.
[15] D. L. Fanselow, H. G. Drickamer, *J. Chem. Phys.* **1974**, *61*, 4567 – 4574.
[16] a) D. H. Evans, R. W. Busch, *J. Am. Chem. Soc.* **1982**, *104*, 5057 – 5062; b) Y. Cohen, J. Klein, M. Rabinovitz, *J. Chem. Soc. Chem. Commun.* **1986**, 1071 – 1073; c) M. Jørgensen, K. Lerstrup, P. Frederiksen, T. Bjørnholm, P. Sommer-Larsen, K. Schaumburg, K. Brunfeldt, K. Bechgaard, *J. Org. Chem.* **1993**, *58*, 2785 – 2790.
[17] a) R. H. Cox, *J. Magn. Reson.* **1970**, *3*, 223 – 229; b) M. Walczak, G. D. Stucky, *J. Organomet. Chem.* **1975**, *97*, 313 – 323; c) E. Ahlberg, O. Hammerich, V. D. Parker, *J. Am. Chem. Soc.* **1981**, *103*, 844 – 849; d) P. Neta, D. H. Evans, *J. Am. Chem. Soc.* **1981**, *103*, 7041 – 7045; e) B. A. Olsen, D. H. Evans, *J. Am. Chem. Soc.* **1981**, *103*, 839 – 843; f) B. A. Olsen, D. H. Evans, I. Agranat, *J. Electroanal. Chem.* **1982**, *136*, 139 – 148; g) D. H. Evans, N. Xie, *J. Am. Chem. Soc.* **1983**, *105*, 315 – 320.
[18] W. R. Browne, M. M. Pollard, B. de Lange, A. Meetsma, B. L. Feringa, *J. Am. Chem. Soc.* **2006**, *128*, 12412 – 12413.
[19] a) G. F. Pedulli, *Res. Chem. Intermed.* **1993**, *19*, 617 – 634, and references therein; b) M. F. M. Post, J. Langelaar, J. D. W. Vanvoorst, *Chem. Phys. Lett.* **1977**, *46*, 331 – 333; c) L. Ould-Moussa, O. Poizat, M. Castellá-Ventura, G. Buntinx, E. Kassab, *J. Phys. Chem.* **1996**, *100*, 2072 – 2082; d) M. Castellá-Ventura, E. Kassab, G. Buntinx, O. Poizat, *Phys. Chem. Chem. Phys.* **2000**, *2*, 4682 – 4689; e) M. S. Denning, M. Irwin, J. M. Goicoechea, *Inorg. Chem.* **2008**, *47*, 6118 – 6120; f) E. Gore-Randall, M. Irwin, M. S. Denning, J. M. Goicoechea, *Inorg. Chem.* **2009**, *48*, 8304 – 8316.
[20] D. Eisenberg, A. S. Filatov, E. A. Jackson, M. Rabinovitz, M. A. Petrukhina, L. T. Scott, R. Shenhar, *J. Org. Chem.* **2008**, *73*, 6073 – 6078.
[21] A. Almenningen, O. Bastiansen, L. Fernholt, B. N. Cyvin, S. J. Cyvin, S. Samdal, *J. Mol. Struct.* **1985**, *128*, 59 – 76.
[22] Reduction with lithium metal afforded a species that shows very similar NMR spectra.
[23] A. Minsky, A. Y. Meyer, R. Poupko, M. Rabinovitz, *J. Am. Chem. Soc.* **1983**, *105*, 2164 – 2172.
[24] See the Supporting Information for experimental procedures, NMR spectra of $\mathbf{1}^{2-}$ and $\mathbf{1}^{4-}$, comparison of experimental and calculated ^{13}C NMR spectra, the stereodynamics map with energy values corrected for 298.15 K, and charge distribution of $\mathbf{1}^{2-}$ from natural population analysis.
[25] B. A. Johnson, J. A. Malikayil, I. M. Armitage, *J. Magn. Reson.* **1988**, *76*, 352 – 357.
[26] H. Eyring, *J. Chem. Phys.* **1935**, *3*, 107 – 115.
[27] a) NBO 5.0, E. D. Glendening, K. J. Badenhoop, A. E. Reed, J. E. Carpenter, J. A. Bohmann, C. M. Morales, F. Weinhold, Theoretical Chemistry Institute, University of Wisconsin, Madison, **2001**; b) J. P. Foster, F. Weinhold, *J. Am. Chem. Soc.* **1980**, *102*, 7211 – 7218; c) A. E. Reed, F. Weinhold, *J. Chem. Phys.* **1983**, *78*, 4066 – 4073; d) A. E. Reed, R. B. Weinstock, F. Weinhold, *J. Chem. Phys.* **1985**, *83*, 735 – 746.
[28] C. Bruno, R. Benassi, A. Passalacqua, F. Paolucci, C. Fontanesi, M. Marcaccio, E. A. Jackson, L. T. Scott, *J. Phys. Chem. B* **2009**, *113*, 1954 – 1962.
[29] a) S. W. Staley, C. K. Dustman, K. L. Facchine, G. E. Linkowski, *J. Am. Chem. Soc.* **1985**, *107*, 4003 – 4007; b) P. Boman, B. Eliasson, R. A. Grimm, G. S. Martin, J. T. Strnad, S. W. Staley, *J. Am. Chem. Soc.* **1999**, *121*, 1558 – 1564.

